

FACTORS CONTROLLING THE EFFICIENCIES OF PHOTOINDUCED ELECTRON-TRANSFER REACTIONS

IAN R. GOULD*, JACQUES E. MOSER[†], BRUCE ARMITAGE[‡] and SAMIR FARID*
Research Laboratories, Eastman Kodak Company, Rochester, NY 14650-2109, U.S.A.

Received 11 May 1994; accepted 3 June 1994

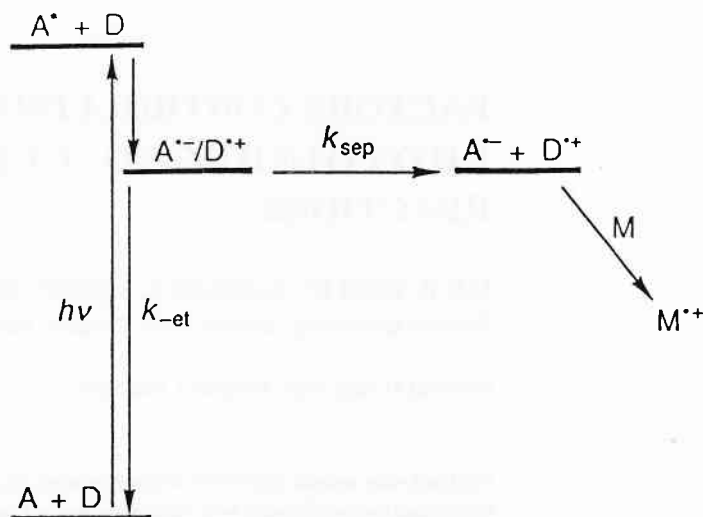
Abstract—The overall efficiencies of photoinduced electron transfer reactions in polar solvents are usually determined by the efficiency with which separated radical ions are formed from the initially formed geminate radical-ion pairs. These separation efficiencies are determined by the competition between return electron transfer and separation within the geminate pairs. A method is described for determining whether variations in the quantum yields for formation of separated radical ions are due to changes in the reorganization parameters for the return electron transfer reactions, or to other factors. The use of the method is illustrated in studies of the effects of varying steric bulk and molecular size of the donors, and also in studies of the effect of using a charged sensitizer.

I. INTRODUCTION

Photoinduced electron transfer reactions are well established as important mechanisms for product formation in photochemical reactions [1]. Photoinduced electron transfer also plays a central role in many processes of technological importance, such as silver halide photography [2a], electrophotography [2b], and photoinduced polymerization [2c]. In the technological applications, it is clearly important that the photoinduced electron transfer processes be efficient, i.e. that as many absorbed photons as possible do useful work. In organic chemical reactions, a corresponding measure of efficiency is the quantum yield for product formation, which ideally should be as high as possible. In most cases, however, quantum yields are usually low, rarely exceeding 5 - 10%, which means that 90 - 95% of the absorbed photons are wasted [3]. The main reason for these low efficiencies can be understood by reference to Scheme I, which illustrates a minimum mechanism for a photoinduced electron transfer process. The Scheme illustrates a common situation for the reaction of a neutral donor and acceptor, where the reaction is carried out in a polar solvent such as acetonitrile. Photoexcitation of, in this example, the electron acceptor (A) to the

[†] *Current Address: Institut de Chimie Physique, Ecole Polytechnique Fédérale, CH-1015, Lausanne, Switzerland.*

[‡] *Current Address: Department of Chemistry, University of Illinois, Urbana, Illinois, U.S.A.*



Scheme I

first excited singlet state (A^*) is followed by exothermic electron-transfer quenching by an electron donor (D) to form a geminate radical-ion pair ($A^{\cdot-} / D^{\cdot+}$). The radical-ion pair either undergoes return electron transfer ($k_{\text{-et}}$) or separation occurs (k_{sep}) to form free radical ions in solution ($A^- + D^{*+}$). In organic systems, chemical reaction products are typical of those of reactions of radical ions in solution [1,3], although in some cases different products have been identified from reactions of the separated radical ions and the geminate radical ion pairs [3]. Whether products are formed within the geminate radical-ion pair, or from reactions of the separated radical ions, however, product formation always competes with the energy-wasting return electron-transfer process ($k_{\text{-et}}$). Clearly it is desirable to understand the factors that control the rate of return electron-transfer reaction so that systems can be designed to maximize the quantum yields for useful chemistry. In fact, in many cases where chain reactions are not involved, the quantum yields for product formation appear to be simply the same as the quantum yields of formation of separated radical ions in solution [4], because when separated, the lifetimes of the radical ions are much longer than within the geminate pairs, and slow reactions can then occur.

Over the last several years we have been studying the factors which control the rates of return electron transfer in the geminate radical-ion pairs [5]. The rates can be understood in terms of current theories of electron-transfer reactions, to the extent that the reactions can actually be used as probes for electron-transfer theories. We have identified several molecular properties which can influence the rates of the return electron-transfer reactions. In this paper we review some of these molecular properties and describe a method for analysis of electron-transfer rate data that can be used to identify which of the factors that control the rates of electron-transfer reactions, if any, are responsible for the observed changes in separation efficiencies.

II. BACKGROUND

Radical-Ion Pairs.

Most photoinduced electron transfer reactions of organic compounds are performed in polar solvents such as acetonitrile, to facilitate separation of the radical ions in the geminate pairs. Two types of geminate radical-ion pair have been identified as playing an important role in photoinduced electron transfer reactions in polar solvents such as acetonitrile, namely the contact radical-ion pair (CRIP, $A^{\cdot-}D^{\cdot+}$) and the solvent separated radical-ion pair (SSRIP, $A^{\cdot-}(S)D^{\cdot+}$) [6]. Return electron transfer can, in principle, occur in both of these radical-ion pairs. In the CRIP, the radical anion and radical cation are assumed to be in face-to-face contact (for flat aromatic systems), with no solvent molecules between the ions [6b]. In the SSRIP, the ions are assumed to have separated to the extent that ca. one layer of solvent molecules separates the ions [6b]. Either a CRIP or a SSRIP may be formed in the bimolecular quenching of the A^* by the D . In acetonitrile, solvation of the CRIP to the SSRIP appears to be fairly rapid [7]. In fact, for most of the acceptor/donor systems studied here, this solvation process appears to be faster than return electron transfer in the CRIP for most of the A/D systems [7]. Furthermore, for those systems in which return electron transfer in the CRIP does compete with solvation, a SSRIP is formed directly in the bimolecular quenching reaction and the CRIP is bypassed [6b]. Therefore, for the bimolecular reactions of the A/D systems studied here in acetonitrile, the energy wasting return electron-transfer reactions are assumed to occur in the SSRIP, and the reactions in the CRIP are not considered.

Theories of Electron-Transfer Rates.

The rates of the return electron-transfer reactions in the SSRIP can be understood in terms of current theories for nonadiabatic electron transfer reactions [8]. In these theories, the rate, k_{et} , is given in the form of a golden rule type expression, i.e. as the product of an electronic coupling matrix element squared (V) and a Franck-Condon weighted density of states (FCWD), Eq. 1 [8]. V measures the extent to which the donor and acceptor interact electronically.

$$k_{et} = V^2 \text{FCWD} \quad (1a)$$

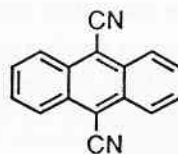
$$\text{FCWD} = f(-\Delta G_{et}, \lambda_s, \lambda_v, \nu_v) \quad (1b)$$

The FCWD contains the dependence of the electron-transfer rate on the driving force, $-\Delta G_{et}$. In a commonly used formalism, the FCWD also includes a reorganization energy associated with rearranged low-frequency (mainly solvent) modes, λ_s , which is treated classically, and a quantized reorganization energy, λ_v , associated with an averaged high frequency mode of frequency ν_v , [8]. When the reaction driving force is less than the total reorganization energy, i.e. $-\Delta G_{et} \leq \lambda_s + \lambda_v$, the reaction becomes faster with increasing

$-\Delta G_{-et}$ (Marcus normal region behavior) [8c]. When the $-\Delta G_{-et}$ approaches $\lambda_s + \lambda_v$, the reaction rate reaches a maximum, and when $-\Delta G_{-et}$ is larger than $\lambda_s + \lambda_v$, the reaction rate decreases with further increases in $-\Delta G_{-et}$ (Marcus inverted region behavior) [8c]. The effect of quantization of the high frequency modes associated with λ_v is that the increase in the rate constant for electron transfer in the normal region is steeper than the decrease in the rate constant in the inverted region. The effect of increasing λ_s or λ_v is to increase the value of $-\Delta G_{-et}$ required to achieve the maximum rate. Increasing λ_v also results in a less pronounced decrease in rates in the inverted region. Increasing ν_v also results in a less pronounced decrease in the inverted region. The effect of increasing V is to increase the reaction rate at all values of $-\Delta G_{-et}$, since V is simply a scaling factor for the rates, Eq. 1.

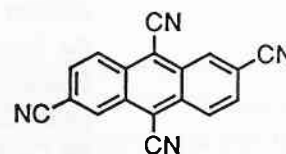
Experiments

In the experiments described here the reactions of the radical-ion pairs are compared to those of a reference set of radical-ion pairs. In the reference set the electron acceptors are 9,10-dicyanoanthracene (DCA) and 2,6,9,10-tetracyanoanthracene (TCA).



DCA

-0.91



TCA

-0.44

E_A^{red}
V vs SCE

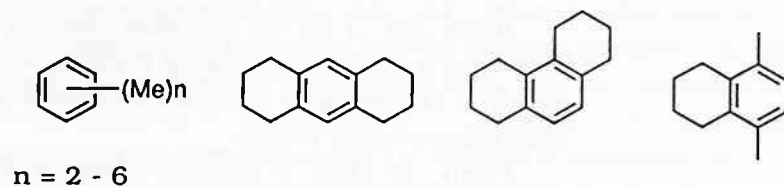
TCA is easier to reduce than DCA by 0.47 V [5d]. The electron donors in the reference set are the simple alkyl-substituted benzenes shown in Scheme II. With increasing alkyl-substitution, the oxidation potentials of the benzene donors decrease (Scheme II). The driving force associated with the return electron-transfer reactions in the SSRIP in acetonitrile, $-\Delta G_{-et}$, is given simply by Eq. 2 [5d].

$$-\Delta G_{-et} = E_D^{\text{ox}} - E_A^{\text{red}} \quad (2)$$

Therefore by changing the donor/acceptor combination within this homologous series, the exothermicity of the return electron-transfer reaction can be varied over a range of ca. 0.8 V.

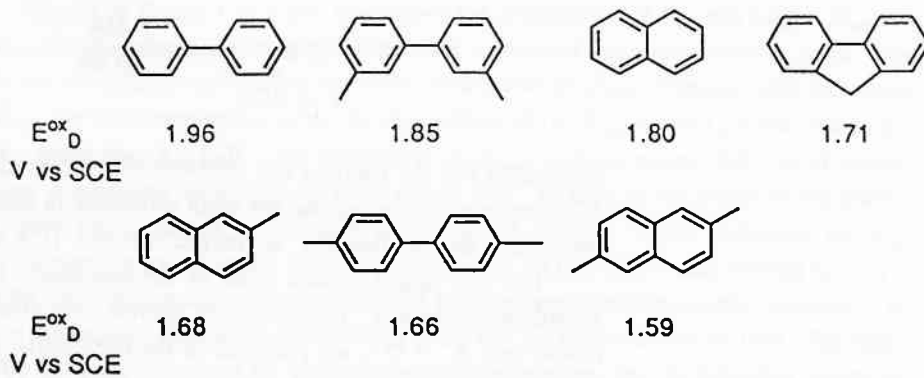
The effects of changing molecular size are investigated by comparing the reference set to radical-ion pairs with the alkyl-substituted naphthalenes and related 2-aromatic ring compounds as donors as shown in Scheme III.

The effects of varying steric bulk are investigated by studying radical-ion pairs of the donors shown in Schemes IV and V.

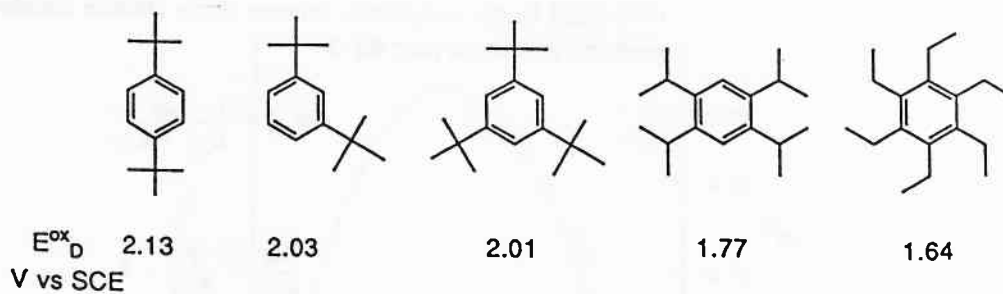


E^{ox}_{D} 1.59 - 2.14
V vs SCE

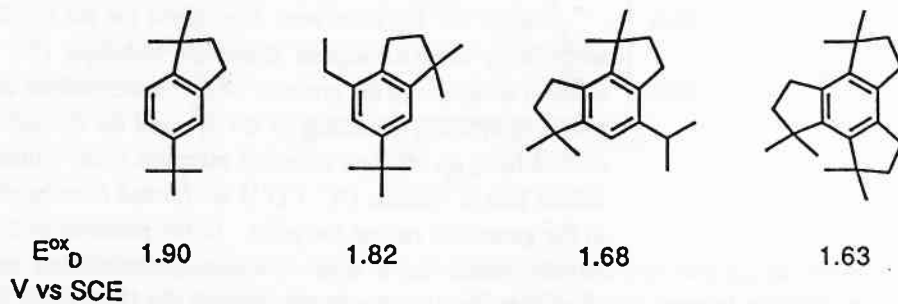
Scheme II



Scheme III



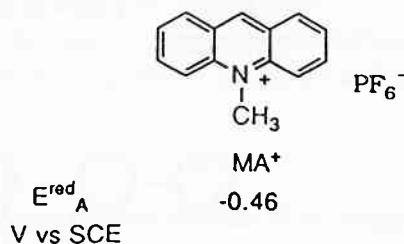
Scheme IV



Scheme V

Within each of the sets of donors, structural changes are minimized so that a homologous series of electron-transfer reactions can be studied. Within each series, the main effect of changing the donors and the acceptor is to change the driving force for the return electron-transfer reaction.

Finally, the effect of molecular change is also investigated by comparing N-methylacridinium (MA^+) as the excited state sensitizer with TCA. The molecular



dimensions and the energies and lifetimes of the first excited singlet states of MA^+ and TCA are very similar, so that the main difference in their photoinduced electron-transfer reactions is the fact that MA^+ is charged, whereas TCA is neutral.

The first singlet excited states of the sensitizers, A^* , are quenched by the donors according to Scheme I. The quantity of interest is the efficiency, Φ_{sep} , with which separated radical ions $\text{A}^{\cdot-} + \text{D}^{\cdot+}$, are produced in the bimolecular electron-transfer reaction. (This discussion assumes a neutral acceptor, i.e. DCA or TCA. When MA^+ is used as the acceptor a neutral radical and a radical cation will be formed, see further below). Φ_{sep} is determined by the competition between return electron transfer and separation within the geminate radical-ion pair, Eq. 3.

$$\Phi_{\text{sep}} = \frac{k_{\text{sep}}}{k_{\text{sep}} + k_{-\text{et}}} \quad (3a)$$

$$\frac{k_{-\text{et}}}{k_{\text{sep}}} = \frac{1}{\Phi_{\text{sep}}} - 1 \quad (3b)$$

Values for Φ_{sep} have been determined for the reaction of the A^* with various D in acetonitrile, using a transient absorption technique [5d]. Pulsed laser photolysis of the electron acceptors in the presence of D (concentrations varied from ca. 0.02 M to 0.2 M), results in efficient quenching of the A^* , and the formation of $\text{A}^{\cdot-} / \text{D}^{\cdot+}$. For the systems studied here, no efficient chemical reactions occur within the radical ion pair. Separated radical ions in solution ($\text{A}^{\cdot-} + \text{D}^{\cdot+}$) are formed in competition with return electron transfer in the geminate radical-ion pairs. In the presence of 5×10^{-4} M, 4,4'-dimethoxystilbene (DMS), which has a lower oxidation potential than any of the D used in this work, secondary electron transfer occurs from the DMS to the separated donor radical cations to form the $\text{DMS}^{\cdot+}$. The DMS acts as a "monitor" (M, Scheme I) for the separated radical

cations. The optical absorption of the $\text{DMS}^{+\cdot}$ ($\text{M}^{+\cdot}$, Scheme I) radical cation at 530 nm can easily be detected by using conventional transient absorption techniques [5d]. The amount of the $\text{DMS}^{+\cdot}$ cation observed is related directly to Φ_{sep} , since the concentration of the DMS is sufficient to trap all of the separated $\text{D}^{+\cdot}$. Corrections were made for incomplete interception of the A^* , from measurements of the extent of fluorescence quenching in the presence of the donors. In some cases, the Φ_{sep} depended upon the concentration of the donors (Φ_{sep} decreasing with increasing [D]). In these cases, the Φ_{sep} were extrapolated to zero donor concentration, again after correcting for incomplete interception of the A^* . The measured Φ_{sep} vary over a wide range for the A/D pairs studied here, from as high as ca. 0.7 to as low as ca. 0.02. Once the Φ_{sep} are known, values for the rate ratio $k_{\text{et}}/k_{\text{sep}}$ for the various radical-ion pairs can be easily obtained using Eq. 3b.

Shown in Figure 1 is a plot that shows the dependence of Φ_{sep} and $\text{Log}(k_{\text{et}}/k_{\text{sep}})$ on $-\Delta G_{\text{et}}$ for the reference cyanoanthracene/alkyl substituted benzene radical-ion pairs. The data are remarkably scatter free and show clearly that $(k_{\text{et}}/k_{\text{sep}})$ decreases with increasing $-\Delta G_{\text{et}}$. For this homologous series, the dependence of $(k_{\text{et}}/k_{\text{sep}})$ on $-\Delta G_{\text{et}}$ is due to changes in k_{et} rather than k_{sep} [5d]. The decrease in $(k_{\text{et}}/k_{\text{sep}})$ with increasing $-\Delta G_{\text{et}}$ is, of course, a clear example of the Marcus inverted region [5d]. In fact, in the course of our studies we have found that it is the driving force that has the largest influence on Φ_{sep} . Nevertheless, other molecular factors influence Φ_{sep} , so that at the same driving force Φ_{sep} can be quite different for different types of photoinduced electron-transfer reaction. The curve through the data points is calculated using Eq. 1, as described in ref [6b]. The shape of the curve is determined by the reorganization parameters, and the following values are used: 1.72 eV for λ_s , 0.20 eV for λ_v , and 1400 cm^{-1} for ν_v . The vertical displacement of the

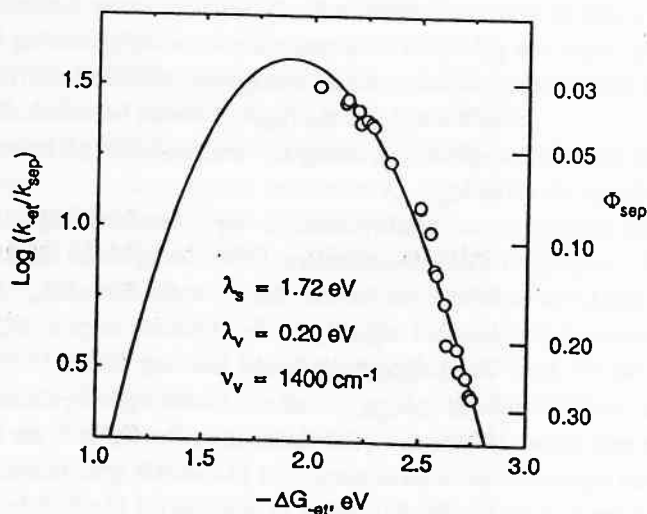


Figure 1. Plot of (left axis) the logarithm of the rate ratio $(k_{\text{et}}/k_{\text{sep}})$ and (right axis) Φ_{sep} , as a function of driving force, $-\Delta G_{\text{et}}$, for the return electron-transfer reactions in the solvent-separated radical-ion pairs of cyanoanthracene radical anions and the simple alkylbenzene radical cations shown in Scheme II.

curve is determined by the values used for V and k_{sep} . For these types of radical-ion pairs in acetonitrile k_{sep} has been estimated to be ca. $5 - 8 \times 10^8 \text{ s}^{-1}$ [5d,7]. Assuming that k_{sep} is constant for the structurally related radical-ion pairs, a value of $10.8 - 13.7 \text{ cm}^{-1}$ for V is required to correctly reproduce the vertical displacement of the data.

In this paper, the separation yields are determined for the SSRIP of the different sets of radical-ion pairs discussed above. For the different systems studied, the rate ratio (k_{et}/k_{sep}) is compared to the corresponding ratio for the reference cyanoanthracene/alkyl substituted benzene pairs. For proper comparison, the rate ratios have to be compared at the same $-\Delta G_{et}$. Therefore, the rate ratios for the different SSRIP are compared to calculated reference (k_{et}/k_{sep}) values for the reference pairs, referred to as $(k_{et}/k_{sep})_{ref}$, with these reference values calculated using the parameters used to calculate the curve through the data shown in Figure 1.

III. DISCUSSION

Molecular Size Effect

The Φ_{sep} were measured for the substituted two-ring donors of Scheme III [5d]. For these reactions, the Φ_{sep} , and thus the (k_{et}/k_{sep}), decrease with increasing $-\Delta G_{et}$, in a similar manner to the reference pairs of Figure 1. However, at similar $-\Delta G_{et}$, the Φ_{sep} when using the two-ring donors are larger than the Φ_{sep} for the reference pairs [5d]. Evidently, either the k_{sep} or the k_{et} are different for the SSRIP involving the two-ring donors compared to the one-ring donors. Differences in the reorganization parameters λ_s , λ_v or ν_v should manifest themselves in changes in the driving force dependence of k_{et} , as discussed above. If V is different for the reactions of the two types of SSRIP, the driving force dependence should be the same, since V is simply a scaling factor for k_{et} (see above). Similarly, if k_{sep} is different for the two types of SSRIP, the driving force dependence of (k_{et}/k_{sep}) should be unaffected, but the (k_{et}/k_{sep}) should be scaled. Therefore, from studies of the driving force dependence, changes in reorganization parameters can be distinguished from changes in V or k_{sep} .

A fairly sensitive way to test for changes in the driving force dependence for two sets of electron-transfer reactions is to plot the electron-transfer rate data for one set of reactions versus that for the other set at the same ΔG_{et} . For data that is only in either the normal or inverted regions, and over a limited range of ΔG_{et} , such a plot will be approximately linear. The $\text{Log}(k_{et}/k_{sep})$ for the two-ring donors is shown plotted versus the corresponding ratio $\text{Log}(k_{et}/k_{sep})_{ref}$ calculated for the one-ring donors at the same $-\Delta G_{et}$, as discussed above, in Figure 2. Also included in the figure is an identity line with a slope of unity and an intercept of zero. In a plot of this type, points will fall on the identity line if the (k_{et}/k_{sep}) for the data points in question are identical to the ($k_{et}/k_{sep})_{ref}$. If the data points define a line that has a different slope than the identity line, then the reorganization parameters for the return electron transfer reactions of the donors in question are different from those for the reference pairs. If the data points define a line that has the same slope as the identity line, but is displaced from it, then there is a constant difference in the rates of (k_{et}/k_{sep}) and

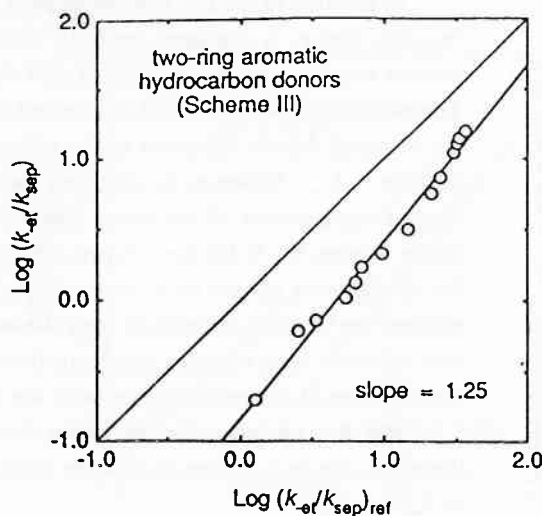


Figure 2. Plot of the logarithms of the rate ratios (k_{-et}/k_{sep}) for return electron-transfer in radical-ion pairs derived from cyanoanthracene acceptors and the two-ring aromatic hydrocarbon donors (Scheme III) versus the logarithms of the corresponding rate ratios calculated at the same $-\Delta G_{et}$ for reference radical-ion pairs derived from cyanoanthracene acceptors and the donors shown in Scheme II. The thin line has a slope of unity and an intercept of zero.

(k_{-et}/k_{sep})_{ref} as a function of $-\Delta G_{et}$. For example, there might be a difference in V for the two data sets. For all the radical-ion pairs discussed here, the return electron transfer reactions are in the inverted region. Therefore, when data points lie below the identity line (whether the slope is larger or smaller than unity), the Φ_{sep} are larger than those of the corresponding reference pairs, and when data points lie above the identity line, the Φ_{sep} are smaller and formation of separated radical ions is less efficient.

The slope of the plot in Figure 2 is greater than unity, 1.25, which confirms the fact that at least one of the reorganization parameters λ_s , λ_v or ν_v for the naphthalene donors is less than that for the benzene donors. An estimate of the extent to which the reorganization parameters change can be obtained by simulating the slope of the plot. This is done by determining the values of reorganization parameters required so that a plot of a calculated set of $\text{Log}(k_{-et}/k_{sep})$ versus the $\text{Log}(k_{-et}/k_{sep})_{ref}$ has the same slope as the actual plot. Indeed, the slope of the line of Figure 2 can be reproduced using 1.59 for λ_s for the two-ring donor data, with λ_v and ν_v being the same as for the reference donors (0.2 eV and 1400 cm^{-1}). Actually, it is not possible to determine whether the two-ring donors have a smaller λ_s , λ_v or ν_v in this way. For the purposes of the present discussion it is simply assumed here that the λ_v and ν_v are the same for both sets of donors. A decrease in λ_s is reasonable however, since the increased delocalization of the positive charge in the two-ring donors might reasonably be expected to result in decreased solvation, and hence a smaller λ_s .

In addition to the fact that the slope is greater than unity, the plot of the data for the two-ring donors is displaced vertically downwards compared to the identity line. The vertical displacement of the type of plot shown in Figure 2 is determined by (V^2/k_{sep}) . Therefore, it cannot actually be determined whether this displacement of the data points for the two-ring donors compared to the reference donors is due to a decrease in V , or an increase in k_{sep} . However, by assuming that k_{sep} for the two sets of data are the same, the vertical displacement of the actual line corresponding to the data can be reproduced by taking a value for V for the two-ring data which is smaller than the corresponding value for the benzene donors by a factor of ca. 0.75. A smaller electronic coupling matrix element can be easily understood since the molecular orbitals of the larger two-ring radicals ions will have more complex nodal structures than those of the simple benzene donors, and thus the overall electronic overlap with the radical anion will be smaller.

The Φ_{sep} are larger for the 2-ring donors compared to the reference 1-ring donors therefore, due to a change in *both* the reorganization parameters, and also a change in V or k_{sep} .

Steric Crowding Effect

Experiments were performed using the sterically-hindered benzene donors as shown in Schemes IV and V [5h]. The results of these experiments are illustrated in Figures 3 and 4, as plots of $\text{Log}(k_{et}/k_{sep})$ versus $\text{Log}(k_{et}/k_{sep})_{ref}$, as before. For the sterically-hindered donors, two groups can be clearly identified as shown in Schemes IV and V. For the donors of Scheme IV (Figure 3), the slope is greater than unity, 1.25, which clearly indicates that the reorganization parameters for these donors are less than for the noncrowded reference donors. For the donors of Scheme V (Figure 4), the slope of the plot is very close to unity, 1.03, but is displaced vertically below the identity line. The fact that all the data points for both groups of sterically-hindered donor lie below the identity line clearly shows that the efficiency of formation of separated radical ions is larger for both groups. The fact that the two plots have different slopes is interesting. The donors of Scheme V, (for which the slope of the plot shown in Figure 4 is close to unity), are dimethylindan type donors. Those for which the slope is greater than unity have *tert*-butyl, *ortho*-*iso*-propyl and *ortho*-ethyl groups (Scheme IV). The steric effect of these *ortho*-groups on tetra-*iso*-propylbenzene and hexaethylbenzene (Scheme IV) are similar to the *tert*-butyl groups on the other donors. The steric crowding forces methyl groups above and below the plane of the ring in both cases. One obvious difference between the two groups of sterically-hindered donors is that the dimethylindan compounds (Scheme V) have hydrogens α to the benzene ring, that are fixed in an orientation to facilitate hyperconjugation stabilization of the radical cation (i.e. above and below the plane of the benzene ring). The donors in Scheme IV, however, either have no α hydrogens, or the α hydrogens are fixed in a position so that hyperconjugation stabilization in the radical cation will be minimized (i.e. in the plane of the benzene ring). Hyperconjugation delocalizes the positive charge in the radical cation into the alkyl substituents. Thus, vibrational modes associated with the substituents will have lower frequency in they involve alkyl groups

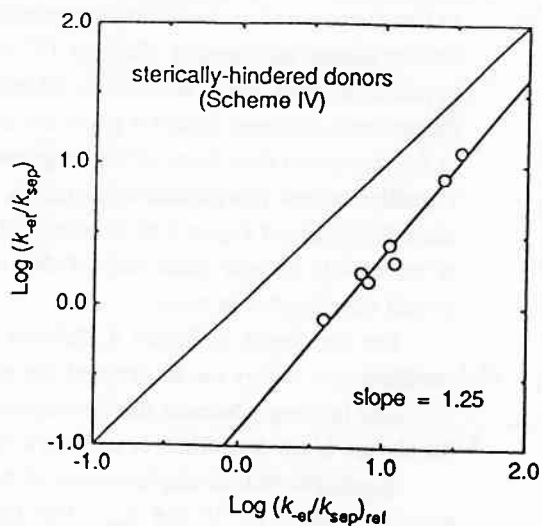


Figure 3. Plot of the logarithms of the rate ratios (k_{et}/k_{sep}) for return electron-transfer in radical-ion pairs derived from cyanoanthracene acceptors and sterically-hindered donors shown in Scheme IV versus the logarithms of the corresponding rate ratios calculated at the same $-\Delta G_{et}$ for reference radical-ion pairs derived from cyanoanthracene acceptors and the donors shown in Scheme II. The thin line has a slope of unity and an intercept of zero.

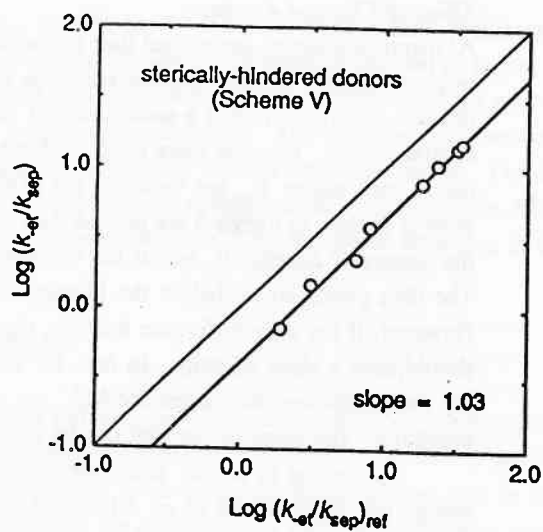


Figure 4. Plot of the logarithms of the rate ratios (k_{et}/k_{sep}) for return electron-transfer in radical-ion pairs derived from cyanoanthracene acceptors and sterically-hindered donors shown in Scheme V versus the logarithms of the corresponding rate ratios calculated at the same $-\Delta G_{et}$ for reference radical-ion pairs derived from cyanoanthracene acceptors and the donors shown in Scheme II. The thin line has a slope of unity and an intercept of zero.

(Scheme IV donors) compared to hydrogens (Scheme V donors). This is a similar situation to that encountered in deuterium isotope effect experiments [5b]. Simulations of the slope for the donors of Figure 3 (Scheme IV) indicate that more than just a change in ν_v is required, however, and a decrease in the total reorganization energy is also necessary. For the sterically-hindered donors it might not be surprising if the radical cations were solvated to a lesser extent than those of the noncrowded donors, which would presumably result in a smaller solvent reorganization energy, λ_s . However, it is also possible to simulate the slope for donors of Figure 3 by decreasing λ_s , and so from this data alone it is not possible to say exactly by how much each of the reorganization parameters decrease, just that an overall decrease has to occur.

For the donors of Figure 4 (Scheme V), it is surprising that no change in solvent reorganization energy can be detected (the slope of the plot of Figure 4 is essentially unity). This may be simply because the dimethylindan donors are somewhat less crowded, and so the change is not detectable, or perhaps a corresponding increase occurs in either λ_s or ν_v .

Again, the vertical displacements of the plots in Figures 3 and 4 can be simulated by assuming values for V and k_{sep} . For both sets of donors, the displacements can be reproduced by using a value for V that is smaller than the value for the reference benzene donors by a factor of 1.5. For these donors, a decrease in V is easily understood as arising from the increased separation of the radical anion and radical cation in the SSRIP as a result of the increased steric bulk on the donors [5h].

Effect of Charged Acceptor

As mentioned above, the excited state properties of N-methylacridinium (MA^+) with respect to photoinduced electron-transfer reactions are very similar to those of TCA. The most obvious difference is that a radical/radical cation pair is formed when MA^{+*} reacts with neutral donors. Because there is no coulombic barrier to separation in the radical/radical cation pair, higher Φ_{sep} are expected for MA^+ compared to TCA. In fact, that is exactly what is found. In Figure 5 are plotted the $\text{Log}(k_{et}/k_{sep})$ data for the reactions of MA^+ with the donors of Scheme II, versus the corresponding $\text{Log}(k_{et}/k_{sep})_{ref}$ values as before [5c]. The data points all lie below the identity line, due to the larger Φ_{sep} when using MA^+ . However, if the only difference between the two sets of reactions were k_{sep} , then the line should have a slope of unity. In fact, the slope is 1.46 which shows that one or more of the reorganization parameters for MA^+ are smaller than for the neutral cyanoanthracene acceptors. The slope of the plot can be reproduced using a value of 1.52 for λ_s .

According to simple dielectric continuum theories for the solvent reorganization energy [9], there should be no difference in λ_s for the charged and uncharged acceptors, since the number of transferred charges is the same in each case. The return electron-transfer reactions in the radical-ion pairs are charge recombination processes, whereas return electron transfer in the radical/radical cation pairs are charge shift processes (i.e. there is no net change in charge). It has been suggested that the driving force dependence might be different for these different types of electron-transfer reactions, due to solvent saturation effects [10]. According to this model, for reactions in the inverted region, the dependence

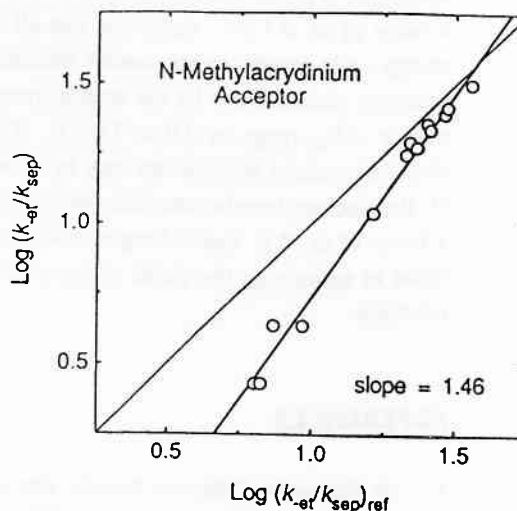


Figure 5. Plot of the logarithms of the rate ratios (k_{et}/k_{sep}) for return electron-transfer in radical/radical-cation pairs derived from N-methylacridinium as the acceptor and the substituted benzene donors shown in Scheme II versus the logarithms of the corresponding rate ratios calculated at the same $-\Delta G_{et}$ for reference radical-ion pairs derived from cyanoanthracene acceptors and the same donors. The thin line has a slope of unity and an intercept of zero.

of rate on ΔG_{et} should be weaker for charge shift processes compared to charge recombination processes. However, the slope of the plot in Figure 5 is greater than unity, which indicates that the charge shift reactions actually exhibit a *greater* dependence on ΔG_{et} than the charge recombination reactions. The differences in the reorganization parameters are therefore inconsistent with the solvent saturation model. The differences may simply indicate that the structures of the radical/radical cation pairs are different from the radical-ion pairs, as a consequence of the lack of coulombic attraction in the former.

IV. CONCLUSIONS

Although the largest influence on the quantum yields for the formation of separated radical ions in bimolecular photoinduced electron-transfer reactions in solution is the driving force for return electron transfer, other molecular properties can also be manipulated to increase the yields. In this work, the advantages of increased molecular size and steric bulk in the donors, and the use of a positively charged acceptor in increasing the yields of separated radical ions are demonstrated. From plots of the logarithms of the return electron-transfer rates versus the corresponding rates for reference systems, it is possible to determine to what extent these changes in yields are due to changes in electron-transfer reorganization parameters, or other factors such as the extent of electronic coupling. For the present

systems it is found that the reorganization energy for return electron transfer can vary over a range of ca. 0.3 eV. Assuming that all of the changes are in the solvent reorganization energy, this results in substantial decreases in the return electron-transfer rate for the reactions characterized by the smaller reorganization energy, by factors of ca. 2 to ca. 20 over a $-\Delta G_{et}$ range of 2.0 to 3.0 eV. For the present systems it is estimated that the electronic matrix element can vary by a factor of ca. 1.5. This means that for the smaller V , the electron-transfer rates are decreased by the square of this value at all $-\Delta G_{et}$, i.e. by a factor of ca. 2.3. Such changes in the return electron-transfer rates can be of substantial value in optimizing the yields of separated radical ions in photoinduced electron-transfer reactions.

REFERENCES

1. a) *Photoinduced Electron Transfer, Part C. Photoinduced Electron-Transfer Reactions: Organic Substrates*, M.A. Fox and M. Chanon (Eds.), Elsevier, Amsterdam, (1988); b) G.J. Kavarnos and N.J. Turro, *Chem. Rev.*, **86**, 401 (1986); c) S.L. Mattes and S. Farid. In: *Organic Photochemistry*, A. Padwa (Ed.), Marcel Dekker, New York, **6**, 233 (1983).
2. a) H.T. James. In: *Advances in Photochemistry*, D.H. Volman, K. Gollnick and G.S. Hammond (Eds.), Wiley, New York, **13**, 329 (1986); b) J.H. Perlstein and P.M. Borsenberger. In: *Extended Linear Chain Compounds*, J.F. Miller (Ed.), Plenum, New York, **2**, Chapter 8 (1982); c) D.F. Eaton. In: *Advances in Photochemistry*, D.H. Volman, K. Gollnick and G.S. Hammond (Eds.), Wiley, New York, **13**, 427 (1986).
3. see for example: a) S.L. Mattes and S. Farid, *J. Chem. Soc. Chem. Commun.*, 126 (1980); b) S.L. Mattes and S. Farid, *J. Am. Chem. Soc.*, **105**, 1386 (1983); c) S.L. Mattes and S. Farid, *J. Am. Chem. Soc.*, **108**, 7356 (1986).
4. see for example: F.D. Lewis, A.M. Bedell, R.E. Dykstra, J.E. Elbert, I.R. Gould and S. Farid, *J. Am. Chem. Soc.*, **112**, 8055 (1990).
5. a) I.R. Gould, J.E. Moser, D. Ege and S. Farid, *J. Am. Chem. Soc.*, **110**, 1991 (1988); b) I.R. Gould and S. Farid, *J. Am. Chem. Soc.*, **110**, 7883 (1988); c) I.R. Gould, J.E. Moser, B. Armitage, S. Farid, J.E. Goodman and M.S. Herman, *J. Am. Chem. Soc.*, **111**, 1917 (1989); d) I.R. Gould, D. Ege, J.E. Moser and S. Farid, *J. Am. Chem. Soc.*, **112**, 4290 (1990); e) I.R. Gould, R.H. Young and S. Farid. In: *Photochemical Processes in Organized Molecular Systems*, K. Honda (Ed), Elsevier, Amsterdam, (1991); f) I.R. Gould, L.J. Mueller and S. Farid, *Z. Phys. Chem. (Munich)*, **170**, 143 (1991); g) I.R. Gould and S. Farid, *J. Am. Chem. Soc.*, **115**, 4814 (1993); h) I.R. Gould and S. Farid, *J. Phys. Chem.*, **97**, 13067 (1993).
6. a) A. Weller, *Z. Phys. Chem. (Munich)*, **130**, 129 (1982); b) I.R. Gould, R.H. Young and S. Farid, *J. Phys. Chem.*, **95**, 2068 (1991).
7. I.R. Gould and S. Farid, *J. Phys. Chem.*, **96**, 7635 (1992).
8. a) J. Ulstrup and J. Jortner, *J. Chem. Phys.*, **63**, 4358 (1975); b) J.R. Miller, J.V. Beitz and R.K. Huddleston, *J. Am. Chem. Soc.*, **106**, 5057 (1984); c) R.A. Marcus and N. Sutin, *Biochim. Biochim. Acta*, **811**, 265 (1985).
9. R.A. Marcus, *Annu. Rev. Phys. Chem.*, **15**, 155 (1964).
10. T. Kakitani and N. Nataga, *J. Phys. Chem.*, **91**, 6277 (1987).